



Published in final edited form as:

Gene Ther. 2017 January ; 24(1): 31–39. doi:10.1038/gt.2016.73.

Effect of Sustained PDGF Non-Viral Gene Delivery on Repair of Tooth-Supporting Bone Defects

Alexandra B. Plonka¹, Behnoush Khorsand², Ning Yu¹, James V. Sugai¹, Aliasger K. Salem^{2,3}, William V. Giannobile^{1,4}, and Satheesh Elangovan³

¹Department of Periodontics and Oral Medicine, University of Michigan School of Dentistry, 1011 N. University Ave., Ann Arbor, MI 48109-1078 USA

²Division of Pharmaceutics and Translational Therapeutics, The University of Iowa College of Pharmacy, 115 S. Grand Avenue, S228 PHAR, Iowa City, Iowa – 52242, USA

³Department of Periodontics, The University of Iowa College of Dentistry & Dental Clinics, 801 Newton Road, Iowa City, Iowa 52242

⁴Department of Biomedical Engineering, University of Michigan College of Engineering, 1221 Beal Avenue, Ann Arbor, MI 48109-2102 USA

Abstract

Recombinant human platelet-derived growth factor-BB (rhPDGF-BB) promotes soft tissue and bone healing, and is FDA-approved for treatment of diabetic ulcers and periodontal defects. The short half-life of topical rhPDGF-BB protein application necessitates bolus, high-dose delivery. Gene therapy enables sustained local growth factor production. A novel gene activated matrix delivering polyplexes of polyethylenimine (PEI)-plasmid DNA (pDNA) encoding PDGF was evaluated for promotion of periodontal wound repair *in vivo*. PEI-pPDGF-B polyplexes were tested in human periodontal ligament fibroblasts (hPLFs) and gingival fibroblasts (hGFs) for cell viability and transfection efficiency. Collagen scaffolds containing PEI-pPDGF-B polyplexes at two doses, rhPDGF-BB, PEI-vector, or collagen-alone were randomly delivered to experimentally-induced tooth-supporting periodontal defects in a rodent model. Mandibulae were harvested at 21-days for histologic observation and histomorphometry. PEI-pPDGF-B polyplexes were biocompatible to cells tested and ELISA confirmed the functionality of transfection. Significantly greater osteogenesis was observed for collagen-alone and rhPDGF-BB versus the PEI-containing groups. Defects treated with sustained PDGF gene delivery demonstrated delayed healing coupled with sustained inflammatory cell infiltrates lateral to the osseous defects. Continuous PDGF-BB production by non-viral gene therapy could have delayed bone healing. This non-viral gene delivery system in this model appeared to prolong inflammatory response, slowing alveolar bone regeneration *in vivo*.

Users may view, print, copy, and download text and data-mine the content in such documents, for the purposes of academic research, subject always to the full Conditions of use: http://www.nature.com/authors/editorial_policies/license.html#terms

Corresponding author: Satheesh Elangovan, BDS, DSc, DMSc, Associate Professor, Department of Periodontics, The University of Iowa College of Dentistry & Dental Clinics, 801 Newton Road, Iowa City, Iowa 52242, TEL: 319-335 7543, satheesh-elangovan@uiowa.edu.

CONFLICT OF INTEREST

The authors report no conflict of interest related to the work presented in this article.

Keywords

platelet-derived growth factor; gene therapy; periodontal regeneration; wound repair; tissue engineering; regenerative medicine

INTRODUCTION

Periodontal disease, a leading cause of tooth loss, is a chronic inflammatory condition afflicting nearly half the adult population in the United States¹. Periodontitis is initiated by microbial dysbiosis, that drives a host-mediated destruction of the periodontal attachment apparatus, which consists of cementum, periodontal ligament (PDL), and alveolar bone². Current regenerative therapies lack predictability and reproducibility for achieving complete restoration of form and function of lost periodontium, underscoring the need for novel regenerative strategies³.

Tissue engineering approaches combining scaffolding matrices to deliver biomimetic factors, genes, and cells would potentially foster an enhanced environment for regeneration^{4,5}. A key application of this strategy is the use of recombinant human platelet-derived growth factor-BB (rhPDGF-BB), a polypeptide growth factor that is FDA-approved for periodontal regeneration and a potential standard-of-care for periodontal defects^{6,7}. Since its discovery, PDGF has been proven to be a chemotactic and mitogenic activator for gingival fibroblasts, periodontal ligament cells, cementoblasts, and osteoblasts⁷. Yet, limitations of rhPDGF-BB protein delivery include its 30-minute serum half-life, the need for superphysiologic doses for clinical efficacy, and a lack of spatial control within the defect site^{8,9}. Gene therapy would circumvent these challenges by promoting sustained local growth factor production¹⁰.

Traditional gene therapy methods encompass a variety of viral and non-viral strategies. Successful viral gene therapy has been established in systems using retrovirus, adenovirus, adeno-associated virus, and lentivirus vectors, among others.¹¹ In preclinical periodontal defect models, adenovirus-encoding PDGF-B has shown effectiveness in stimulating regeneration of periodontal attachment^{12,13}. In a phase I clinical trial, adenovirus encoding PDGF-B was administered directly to leg wound edges and patients displayed markedly improved healing without any apparent clinical safety issues¹⁴. Even though viral approaches are promising, perceived safety concerns pose a challenge for human translation for treatment of non-life-threatening conditions¹⁵. Non-viral gene delivery systems could overcome this barrier¹⁶. The advantages of non-viral systems include good bioavailability, low cost, ability to carry large DNA segments and minimal induction of host immune responses^{16,17}. An inherent limitation of non-viral gene delivery is a lower transfection efficiency when compared to viral counterparts. Proper selection and optimization of vector-to-DNA ratio significantly enhances non-viral transfection efficiency¹⁶. Our group recently developed a novel non-viral system of polyplexes of PEI-pDNA encoding the PDGF-B gene delivered from collagen matrix. This system demonstrated enhanced bone regeneration when implanted in experimental calvarial bone defects in rats¹⁸. In the present proof-of-concept pilot investigation, we explored the efficacy of the PEI-pPDGF-B containing collagen matrix

for periodontal regeneration in a well-established tooth-associated rat alveolar bone defect model.

RESULTS

Morphology, size and zeta-potential of polyplexes and SEM analysis of collagen scaffolds

The PEI-pPDGF polyplexes at an N/P ratio of 10 were prepared through electrostatic condensation. The polyplexes were 282 ± 16 nm in size with a zeta potential of $+30 \pm 0.5$ mV (Figure 1a). TEM images of these polyplexes showed the formation of discrete, spherical particles with monomodal distribution (Figure 1b). The three-dimensional collagen scaffold was characterized using SEM imaging, which demonstrated a highly interconnecting porous structure (pore diameters ~ 200 μm) (Figure 1c).

Biocompatibility and Transfection Efficiency of PEI-pPDGF polyplexes

Using an MTS cell viability assay, the potential cytotoxic effects of PEI-p*PDGF* polyplexes containing 1 μg of pDNA at a N/P ratio of 10 in hGF and hPLF cells was evaluated after 48 hours. Assay results showed 88% of the hGF and 85% of the hPLF were viable following transfection with PEI-pPDGF polyplexes (Figure 2a and b). The differences in cell viability for the hGF and hPLF cells treated with PEI-pPDGF polyplexes compared to untreated cells were not statistically significant. Significantly lower cell viability was found when evaluating cells treated with PEI versus untreated cells (** $p < 0.01$) and when comparing cells treated with PEI with those treated with PEI-pPDGF-B polyplexes (* $p < 0.05$). PDGF-BB ELISA showed that the hPLF and hGF cells transfected with PEI-pPDGF polyplexes secreted significantly higher levels of protein compared to controls, including cells treated with PEI and untreated cells (**** $p < 0.0001$). This increase in PDGF-BB protein was significant for cells treated with PEI-pPDGF-B when compared to cells treated with PEI and untreated cells at 24 and 48 hours, demonstrating successful functional transfection of hPLF and hGF cells by PEI-pPDGF-B polyplexes (Figure 2C and D).

Descriptive histology

Figure 3 shows representative images (20x) of periodontal defects after 3 weeks of healing (a–e) and higher magnification (100x) views of the prepared tooth-root interface (f–j). Both high- and low-dose PEI-pPDGF-B gene therapy groups and the PEI vector group failed to show bone repair or “bridging” across the defects, while the collagen alone control and rhPDGF-BB groups showed complete bridging of the buccal cortical plate and bone fill within the defects. More limited healing was seen in the gene therapy groups. In the gene therapy and PEI vector groups, a robust inflammatory cell infiltrate was present lateral to the defects. Panels k–o show the histologic features at higher magnification (400x), where residual scaffold and inflammatory cells were present in the PEI and gene therapy groups.

Histomorphometry for measures of periodontal wound repair

Histomorphometric analyses are depicted in Figure 4. Significantly less bridging bone length (4a) and percentage of total length (4b) were found in the PEI-pPDGF-B gene therapy groups and the PEI vector group compared with collagen alone and rhPDGF-BB. There were no statistically significant differences between the PEI-pPDGF-B gene therapy groups

and the PEI vector group, nor was there a difference between the rhPDGF-BB group and collagen alone. No significant differences were found between groups for defect length (Table 1). Similar trends were found for bone area measurements. Significantly less new bone area (4c), as well as the percentage of defect area filled by new bone (4d), was found in the PEI-pPDGF-B gene therapy and PEI vector groups compared with the collagen alone and rhPDGF-BB groups. For total bone area (4e), which is the sum of new bone area within the defect plus bone that formed outside of the prepared defect area, the only deviation from this trend was for the high-dose 50 ug PEI-pPDGF-B gene therapy group, and this was not statistically significantly different than the collagen alone group. However, the high-dose PEI-pPDGF-B gene therapy group showed significantly more cementum formation around the prepared root than all other groups (Table 1).

Quantification of inflammatory cell infiltrate and CD68-positive cell staining

For the PEI-pPDGF-B gene therapy groups and the PEI vector group, a robust inflammatory cell infiltrate was identified in the lateral defect region of the scaffold placement that was not observed in the rhPDGF-BB and collagen groups (Fig 5). These inflammatory cells included lymphocytes, macrophages, and neutrophils. Significantly more inflammatory cells were quantified in the lateral defect region for the PEI-vector and PEI-pPDGF-B gene therapy groups when compared with the control and rhPDGF-BB groups (Figure 5a). Overall, a higher number of inflammatory cells were found in the lateral defect region when compared with the peri-root and peri-defect regions, thus the findings in these regions are most significant. In the peri-root region, inflammatory cells in the PEI-vector group were significantly higher in number than in the collagen alone group. In the peri-defect region, significantly more inflammatory cells were found in the PEI vector group and the 25 µg PEI-pPDGF-B group compared with the collagen alone group. Statistical analysis revealed significantly greater number of inflammatory cells in all PEI-containing groups than the rhPDGF-BB group. To identify and locate inflammatory cells in relation to the defects, immunohistochemistry staining was performed for CD68, a well-characterized marker for macrophages and monocytes and a representative sample from each of the groups (collagen only group, PEI alone, rhPDGF-BB, PEI-pPDGF-B 25µg and PEI-pPDGF-B 50µg) are shown in Figure 5b. As seen, compared to other groups, representative image of a defect implanted with PEI-pPDGF-B 50µg show abundant CD68 positive cells in the lateral area to the bone defect.

DISCUSSION

This study is the first investigation of a novel non-viral gene delivery system of cationic PEI-pDNA encoding PDGF-B polyplexes for its influence on periodontal wound healing. This study is also the first to assess the *in vitro* biocompatibility and transfection potential of PEI-pPDGF-B polyplexes in hGF and hPLF cells. PEI, a cationic polymer is an effective non-viral vector for complexing with, and condensing the DNA and ultimately, enhancing the cellular intake of the resulting polyplexes¹⁹. For this reason, PEI is still considered the ‘gold standard’ for those developing novel non-viral gene delivery vectors. Structurally, PEI can be linear or branched and it was shown that branched PEI, (the one employed in this study) was shown to exhibit stronger electrostatic interaction with DNA, allowing greater

compaction/protection of DNA and thereby reducing the overall size of the polyplexes^{20,21}. PEI as a vector has several advantages including, its established transfection efficiency in numerous cell lines, simple DNA complexation process, stability /shelf life of the resulting complexes and the ability to chemically modify them (especially branched PEI) to enhance transfection²².

In vitro, the PEI-pPDGF-B polyplexes successfully transfected periodontal cells, potentially promoting sustained PDGF-BB production *in vivo* due to the sustained transfection of cells seen when polymer-pDNA or naked pDNA are delivered from a scaffold matrix (termed as 'Gene Activated Matrix') such as collagen.²³ The scaffolds enhance local and long term availability of pDNA at the implanted site for sustained transfection and eventual secretion of target protein for prolonged periods.^{23,24,25} The cellular transfection can occur either by the uptake of pDNA that are released from the collagen matrix (as it disintegrates) or it can occur when the native cells penetrate into the porosities of the collagen matrix and take up the polyplexes presented on the surface of matrix, prolonging the transfection process. Ideally, matrices should be structurally and mechanically stable and should be homogeneously porous with good interconnecting pore structure to allow cells and neo-vasculature to penetrate through. We utilized collagen as our matrix as it satisfies all of the above properties and is also highly biocompatible with a long record of safety in dentistry²⁶. In previous pre-clinical studies testing non-viral gene delivery systems, collagen was used successfully to deliver DNA encoding parathyroid hormone (PTH) 1–34 and/or BMP-4 in a rat femoral and dog tibia bone defects^{27,28}.

In vivo, PEI-pPDGF-B delivery using collagen scaffolds showed significantly less osteogenesis at 3 weeks compared with the collagen-alone or rhPDGF-BB protein groups. Comparing the two doses of PEI-pPDGF-B, the high dose showed slightly more active early bone matrix formation in contrast with the low dose and PEI vector alone groups. A key factor that may have influenced the reduction in bone regeneration by the PEI-pPDGF-B groups may be the dosing profile of PDGF-BB protein. PDGF-BB is naturally released by platelets in response to injury, and acts during the initial inflammatory phase of wound-healing to recruit immune cells for early tissue repair and the formation of new granulation tissue⁸. PDGF-BB also supports bone regeneration by enhancing angiogenesis^{29,30}. Previous reports by our group using adenoviral PDGF-B gene delivery showed that PDGF-BB expression was enhanced for approximately 7 days^{12,31}. While this short-term expression of PDGF has been shown to stimulate periodontal regeneration, a more sustained PDGF delivery *in vivo* might have an inhibitory effect on periodontal healing, since sustained PDGF levels have been associated with chronic inflammation^{32–34}. Elevated PDGF concentrations have also been found adjacent to failing orthopedic and dental implants^{32–34}. PDGF levels were 3 times higher in inflamed gingiva of patients with chronic periodontitis compared with healthy sites³³. Continuous PDGF exposure inhibited osteoblast differentiation and decreased bone nodule formation³⁵. Short doses of PDGF over 1 day during osteoblast differentiation resulted in a significant increase in mineralization *in vitro*^{36,37}. Conversely, sustained PDGF exposure caused less mineralization by inhibiting osteoblast function. The study concluded that several short exposures of PDGF stimulate osteogenesis, while long-term exposure is consistent with chronic inflammation and has a negative effect on mineralization³⁷. Other reports show

bolus administration of PDGF-BB at time of surgery stimulated osteogenesis, while delivery of osteoblast progenitor cells pre-treated with PDGF-BB for prolonged delivery inhibited bone regeneration³⁸. The sustained release of PDGF-BB at the defect site may have turned out to be a disadvantage for this molecule and for this specific defect but sustained delivery of other growth factors or morphogens such as BMP-2 could be advantageous for other applications³⁹. This underscores the importance of custom designing and optimization of the delivery system based on the molecule of interest and for specific clinical applications.

In our present study, a notable inflammatory cell infiltrate was observed lateral to the periodontal defect for both the PDGF gene therapy and PEI vector groups. Other reports confirm that PDGF may stimulate osteoclasts and macrophages and inhibit osteoblasts^{40–42}. In a study of viral PDGF gene delivery, an increased multinucleated giant cell infiltrate and inhibition of cementogenesis was found at 3 weeks *in vivo*, consistent with our study time point⁴³. The release profile of PDGF in gene therapy and other tissue engineering strategies requires optimization for careful temporal control to mimic natural wound healing events.

Finally, this model system, compared with the calvarial model, may be a more representative physiologic environment for evaluation of bone healing. In contrast to the previous calvarial model, which was a critical sized defect (CSD), the periodontal fenestration defect is a kinetic defect^{44,45}. This mandibular defect provides physiologic biomechanical loading forces⁴⁶. Although the calvarium and mandible are similarly formed by intramembranous ossification, periodontal fenestration defects have a unique bone-ligament interface with distinct cell types, such as PDL fibroblasts, cementoblasts, odontoblasts, and osteoprogenitor cells within the PDL space or are recruited from blood. It is possible that an earlier time points would have provided more information on the effects of rhPDGF-BB on early wound healing, and a later time point may have allowed for resolution of inflammation and wound healing, however given the strong response of differences between the controls (PEI vector, collagen alone and PDGF alone versus the 2 gene delivery groups, we feel this study is consistent with a good observational time intervals to assess early alveolar bone regeneration *in vivo* in the rat model^{12,13,47}.

In conclusion, the non-viral PEI-pPDGF-B gene therapy system resulted in effective transfection of hGF and hPLF cells for sustained PDGF-BB production. In periodontal fenestration defects, both non-viral PEI-pPDGF-B gene delivery and the PEI vector control delivery resulted in significantly less bone formation than using collagen alone or rhPDGF-BB protein. Experimental groups containing PEI resulted in a significantly increased number of inflammatory cells in the region lateral to the defect. This investigation revealed that non-viral PEI-pPDGF-B gene therapy may delay periodontal wound healing by prolonging the inflammatory response. This study also provides valuable information for the development of biomaterials for non-viral gene therapy and make available essential data to further optimize the release profile of PDGF-BB for periodontal wound healing.

MATERIALS AND METHODS

In vitro study materials

Branched PEI (mol. wt. 25 kDa) and the GenElute™ HP endotoxin-free plasmid maxiprep kit were purchased from Sigma-Aldrich® (St. Louis, MO). The mouse/rat PDGF Quantikine® ELISA kit was purchased from R&D Systems® (Minneapolis, MN). Plasmid DNA (4.9 Kb) encoding PDGF protein (pPDGF) driven by a CMV promoter/enhancer was obtained from Origene Technologies, Inc. (Rockville, MD). Human periodontal ligament fibroblasts (hPLF) and human gingival fibroblasts (hGF) cells were purchased from American Type Culture Collection (ATCC®, Manassas, VA). Dulbecco's Modified Eagle's Medium (DMEM), trypsin-EDTA (0.25%, 1X solution) and Dulbecco's phosphate buffered saline (PBS) and Penicillin-Streptomycin (10,000 U/mL) were purchased from Gibco® Life Technologies (Grand Island, NY). Fetal bovine serum (FBS) was obtained from Atlanta Biologicals® (Lawrenceville, GA). Absorbable type-I bovine collagen was obtained from Zimmer Dental Inc. (Carlsbad, CA). MTS cell growth assay reagent (Cell Titer 96 AQueous One Solution Cell Proliferation Assay) was purchased from Promega® (Madison, WI). All other chemicals and solvents used were of reagent grade.

Preparation of plasmid DNA (pDNA) encoding PDGF-B

The chemically competent DH5 α ™ bacterial strain (*Escherichia coli* species) was transformed with *pDNA* to amplify the plasmid. The *pDNA* in the transformed cultures was then expanded by amplification of the *E. coli* in Lennox L Broth (LB Broth) overnight at 37°C in a shaking incubator at 300 rpm. Plasmid DNA was extracted using the GenElute™ HP endotoxin-free plasmid maxiprep kit. The purity of the extracted pDNA was analyzed, using a NanoDrop 2000 UV-Vis Spectrophotometer (Thermo Scientific, Wilmington, DE) by measuring the ratio of absorbance (A260/A280 nm). The concentration of *pDNA* solution was determined by absorbance at 260 nm.

Fabrication of PEI-pDNA polyplexes

Polyplexes were prepared by adding 500 μ L PEI solution in water to 500 μ L *pDNA* (PDGF) solution in water containing 50 μ g pDNA and mixed by vortexing for 30 seconds. The mixture was incubated at room temperature for 30 minutes to allow the positively charged PEI (amine groups) and the negatively charged pDNA (phosphate groups) to form polyplexes. In our previous study¹⁷ we found that polyplexes fabricated at N (nitrogen) to P (phosphate) ratios of 10 provides the optimal transfection efficacies. The final volume of the polyplexes utilized for *in vitro* transfection and biocompatibility experiments was 20 μ L, containing 1 μ g pDNA. For the *in vivo* study, PEI-pDNA polyplexes at a N/P ratio of 10 were prepared by mixing 50 μ L PEI solution to 50 μ L pDNA (PDGF) solution¹⁸ containing 25 and 50 μ g pDNA for 30 seconds and subsequently incubated at room temperature for 30 minutes. The polyplexes were then added to the collagen scaffolds and freeze-dried prior to implantation.

Size, zeta-potential, and morphology of the PEI-pDNA polyplexes

Polyplexes in water were characterized for their size and their zeta-potential by using Zetasizer Nano-ZS (Malvern Instruments, Westborough, MA). The particle size and particle size distribution by intensity were measured by photon correlation spectroscopy (PCS), using dynamic laser light scattering (4mW He-Ne laser with a fixed wavelength of 633nm, 173° backscatter at 25°C) in 10 mm-diameter cells. Also the zeta-potential of the polyplexes in water was assessed based on the electrophoretic mobility of the polyplexes, using folded capillary cells, via the Zetasizer Nano-ZS. Zeta potential measurements were performed by the laser scattering method (Laser Doppler Micro-electrophoresis, He-Ne laser, 633 nm, and 17° light scatter at 25°C). All measurements were performed in triplicate. Polyplexes with a N/P ratio of 10 were placed on carbon-formvar coated grids for 1 minute. After drying, the samples were imaged with a JEOL JEM-1230 transmission electron microscopy (TEM).

Collagen scaffold characterization

The surface morphology of the collagen scaffolds was studied using a standard protocol for scanning electron microscopy (SEM) (Hitachi Model S-4800, Japan). Briefly, the scaffolds were mounted on an SEM aluminum stub using double-stick carbon tape, then sputter-coated with gold-palladium by an argon beam K550 sputter-coater (Emitech Ltd., Kent, England). Images were captured using the Hitachi S-4800 SEM operated at 3 kV accelerating voltage and a current of 10 IA.

Cell culture

The hPLF cells were maintained in DMEM supplemented with 10% FBS and 1% Penicillin-Streptomycin (10,000 U/mL) in a humidified incubator (Sanyo Scientific Autoflow, IR direct heat CO₂ incubator) at 37°C containing 95% air and 5% CO₂. The cells were plated and grown as a monolayer in 75 cm² polystyrene cell culture flasks (Corning, NY, USA) and sub-cultured (sub-cultivation ratio of 1:6) after 80–90% confluence was achieved. Cell lines were started from frozen stocks and the media were changed every 2 days. The passage number at which the cells were used in experiments was in the range 4–6.

Viability assay

The MTS cell growth assay (Cell Titer 96 Aqueous One Solution cell proliferation assay, Promega Corporation) was used to determine the cytotoxicity of *PEI-pDNA* polyplexes at an N/P ratio of 10 against hPLF and hGF. Briefly, 10,000 hPLF or hGF cells were seeded in 96-well tissue culture grade plates (Costar®, Corning Inc.) and incubated for 4 hours with polyplexes containing 1 µg of pPDGF. At the end of the incubation period, the cells were washed with 1X PBS and fresh complete medium was added. After a total incubation time of 48 hours, the MTS/PMS reagent was added for 4 hours at 37°C in a humidified 5% CO₂ atmosphere. Absorbance was read at 490nm using SpectraMax® Plus384 (Molecular Devices, Sunnyvale, CA). Percent cell viability was expressed as the ratio of the absorbance intensity of treated cells to absorbance intensity of untreated cells (control) multiplied by 100. Values are expressed as mean ± SD and each treatment was performed in quadruplicate.

In vitro evaluation of the transfection efficacy of PEI-pDNA (PDGF) polyplexes in hPLF and hGF

Cells were seeded at a density of 50,000 cells/well in 24-well plates. The following day, prepared at 80% cell confluency, 20 μ L of polyplexes at an N/P ratio of 10 containing 1 μ g pDNA was added to the serum-free medium. Untreated cells served as a control, and cells treated with PEI alone served as an additional control. At 24 and 48 hours post-transfection, cell supernatants were collected and analyzed using the PDGF ELISA kit, to quantify the amount of PDGF-BB protein secreted into the supernatant. The mean value was recorded as the average of four measurements.

In vivo implantation of complex-embedded collagen scaffolds to periodontal alveolar bone wounds

All animal procedures were performed under the University of Michigan Unit for Laboratory Animal Medicine Guidelines. Animal protocol 4622 was approved by the University Committee on Use and Care of Animals (UCUCA). A periodontal defect was created in alveolar bone through an extra-oral approach, as previously described⁴⁸. In summary, 30 Sprague-Dawley rats (250–300 g; Harlan, Indianapolis, IN, USA) were anesthetized with ketamine and xylazine. The unilateral defects created measured 0.3cm in width x 0.2cm in height and were located in the mandibular buccal plate external to the first and second molar roots. After exposure, the roots were prepared to remove periodontal ligament, cementum, and superficial dentin. Collagen scaffolds containing either the PEI-pPDGF-B complex at a 25 or 50 μ g dose pDNA, PEI vector only (negative control), rhPDGF-BB (GEM21S, Osteohealth Company, Shirley, NY, positive control), or collagen alone (control) was placed into the defect based on random allocation (n = 6 animals/group). Suturing of the muscle (chromic gut; Ethicon, Somerville, NJ, USA) stabilized the scaffold, after which wound clips were used to close the superficial skin incision. Post-operative care included drinking water supplemented with 5% glucose and 268 μ g/mL ampicillin for up to 7 days. At 21 days post-surgery, mandibulae were harvested.

Histologic observation of wound repair

Rat mandibles were placed into 10% formalin fixative (Fisher Scientific, Waltham, MA) and then decalcified in 10% EDTA for 2 to 3 weeks, followed by embedding in paraffin. The specimens were sent to the University of Michigan School of Dentistry Histology Core for 4 to 5 μ m thick sectioning in the coronal plane followed by hematoxylin and eosin (H&E) staining.

Histomorphometric analysis

To evaluate the effect of gene transfer on periodontal repair, digital images of H&E-stained specimens were captured using a Nikon Eclipse E800 microscope (Nikon, Inc., Melville, NY, USA) fitted with a SPOT-2 camera (Diagnostic Instruments, Inc, Sterling Heights, MI, USA) for analysis using NIS-Elements software version BR-3.2 (Nikon Instruments, Inc., Melville, NY, USA). Images were captured at 20, 40, 100, 200, and 400x magnification. A single masked, calibrated examiner (ABP) completed the histomorphometric analysis. The examiner's pre- and post-study calibration inter- and intra-examiner error was <5%

compared to a standard (WVG). The parameters measured included ³⁷: (1) defect length, (2) new bridging bone length (mm), measured from the borders of the surgically-created osseous defect (mesiodistally); (3) bridging bone percentage of defect length, (4) new alveolar bone formed within the defect, (5) alveolar bone defect fill, determined as the percentage of new bone in the original bone defect area excluding the PDL space, (6) length of prepared root surface, and (7) length of new cementum formed along the prepared root surface.

Inflammatory cells quantification and CD68 immunohistochemistry staining

Three regions of interest (ROI) measuring 100 μ m x 200 μ m in size were selected under 200x magnification. The “peri-root” region is defined as the location 50 μ m from the outermost edge of the exposed root. Two “peri-defect” regions were located perpendicular to the edges of the original alveolar bone defects, one on each side of the defect. A fourth region of interest, the “lateral defect” region, was 400 μ m x 200 μ m in size and located 100 μ m away from and perpendicular to an imaginary line created connecting the edges of the defect between the bone defects, directly above the exposed root. Within each ROI, the absolute numbers of infiltrated immune cells (macrophage, polymorphonuclear cell (PMN), and lymphocyte cells) were documented by a calibrated examiner (NY) with ImageJ software version 1.48v⁴⁹. The immune cell quantification for the peri-defect region are reported as the average cell counts from two ROIs. To confirm that these infiltrated cells were indeed immune cells, we examined expression of a CD68 marker by immunohistochemistry staining. Paraffin-embedded sections were deparaffinized and immersed overnight in DIVA solution (Biocare Medical) at 60°C for epitope retrieval. Anti-CD68 antibody (Abcam, ab31630, dilution 1:50) was applied overnight at 4°C followed by the MACH4 HRP-polymer detection system (Biocare Medical). Samples were then treated with DAB (Biocare Medical) and counterstained with hematoxylin. For each section treated with primary antibody, a serial section was treated without primary antibody as the negative control.

Statistical analysis

Statistical analysis was performed using GraphPad Prism version 6.0 for Windows (GraphPad Software Inc., San Diego, CA). One-way analysis of variance (ANOVA) was performed followed by Tukey’s post hoc test to compare all the pairs of treatments and determine the statistical significance. Numerical data are represented as mean \pm SEM and *p*-values less than or equal to 0.05 were considered statistically significant.

Acknowledgments

This study was supported by NIH/NIDCR DE 13397 (WVG), NIH/NIDCR DE024206 (SE and AKS) and the Lyle and Sharon Bighley Professorship (AKS). Authors would like to thank Mr. Anh-Vu Do (University of Iowa College of Pharmacy, Iowa City) for his assistance in plasmids expansion.

References

1. Eke PI, et al. Update on Prevalence of Periodontitis in Adults in the United States: NHANES 2009 to 2012. *J Periodontol.* 2015; 86:611–622. DOI: 10.1902/jop.2015.140520 [PubMed: 25688694]

2. Hajishengallis G. Periodontitis: from microbial immune subversion to systemic inflammation. *Nat Rev Immunol.* 2015; 15:30–44. DOI: 10.1038/nri3785 [PubMed: 25534621]
3. Kao RT, Nares S, Reynolds MA. Periodontal regeneration - intrabony defects: a systematic review from the AAP Regeneration Workshop. *J Periodontol.* 2015; 86:S77–104. DOI: 10.1902/jop.2015.130685 [PubMed: 25216204]
4. Pilipchuk SP, et al. Tissue engineering for bone regeneration and osseointegration in the oral cavity. *Dent Mater.* 2015; 31:317–338. DOI: 10.1016/j.dental.2015.01.006 [PubMed: 25701146]
5. Lin Z, Rios HF, Cochran DL. Emerging regenerative approaches for periodontal reconstruction: a systematic review from the AAP Regeneration Workshop. *J Periodontol.* 2015; 86:S134–152. DOI: 10.1902/jop.2015.130689 [PubMed: 25644297]
6. Nevins M, et al. Platelet-derived growth factor stimulates bone fill and rate of attachment level gain: results of a large multicenter randomized controlled trial. *J Periodontol.* 2005; 76:2205–2215. DOI: 10.1902/jop.2005.76.12.2205 [PubMed: 16332231]
7. Kaigler D, et al. Platelet-derived growth factor applications in periodontal and peri-implant bone regeneration. *Expert Opin Biol Ther.* 2011; 11:375–385. DOI: 10.1517/14712598.2011.554814 [PubMed: 21288185]
8. Hollinger JO, Hart CE, Hirsch SN, Lynch S, Friedlaender GE. Recombinant human platelet-derived growth factor: biology and clinical applications. *J Bone Joint Surg Am.* 2008; 90(Suppl 1):48–54. DOI: 10.2106/JBJS.G.01231 [PubMed: 18292357]
9. Cochran DL, et al. Emerging regenerative approaches for periodontal reconstruction: a consensus report from the AAP Regeneration Workshop. *J Periodontol.* 2015; 86:S153–156. DOI: 10.1902/jop.2015.140381 [PubMed: 25317603]
10. Elangovan S, Karimbux N. Review paper: DNA delivery strategies to promote periodontal regeneration. *Journal of biomaterials applications.* 2010; 25:3–18. DOI: 10.1177/0885328210366490 [PubMed: 20511387]
11. Nayerossadat N, Maedeh T, Ali PA. Viral and nonviral delivery systems for gene delivery. *Adv Biomed Res.* 2012; 1:27. [PubMed: 23210086]
12. Jin Q, Anusaksathien O, Webb SA, Printz MA, Giannobile WV. Engineering of tooth-supporting structures by delivery of PDGF gene therapy vectors. *Mol Ther.* 2004; 9:519–526. DOI: 10.1016/j.yymthe.2004.01.016 [PubMed: 15093182]
13. Chang PC, et al. Adenovirus encoding human platelet-derived growth factor-B delivered to alveolar bone defects exhibits safety and biodistribution profiles favorable for clinical use. *Hum Gene Ther.* 2009; 20:486–496. DOI: 10.1089/hum.2008.114 [PubMed: 19199824]
14. Margolis DJ, et al. Phase I study of H5.020CMV.PDGF-beta to treat venous leg ulcer disease. *Mol Ther.* 2009; 17:1822–1829. DOI: 10.1038/mt.2009.169 [PubMed: 19638959]
15. Evans CH. Gene delivery to bone. *Adv Drug Deliv Rev.* 2012; 64:1331–1340. DOI: 10.1016/j.addr.2012.03.013 [PubMed: 22480730]
16. Luo D, Saltzman WM. Synthetic DNA delivery systems. *Nat Biotechnol.* 2000; 18:33–37. DOI: 10.1038/71889 [PubMed: 10625387]
17. Abbas AO, Donovan MD, Salem AK. Formulating poly(lactide-co-glycolide) particles for plasmid DNA delivery. *J Pharm Sci.* 2008; 97:2448–2461. [PubMed: 17918737]
18. Elangovan S, et al. The enhancement of bone regeneration by gene activated matrix encoding for platelet derived growth factor. *Biomaterials.* 2014; 35:737–747. DOI: 10.1016/j.biomaterials.2013.10.021 [PubMed: 24161167]
19. Lungwitz U, Breunig M, Blunk T, Göpferich A. Polyethylenimine-based non-viral gene delivery systems. *Eur J Pharm Biopharm.* 2005; 60:247–266. [PubMed: 15939236]
20. Intra J, Salem AK. Characterization of the transgene expression generated by branched and linear polyethylenimine-plasmid DNA nanoparticles in vitro and after intraperitoneal injection in vivo. *J Control Release.* 2008; 130:129–138. DOI: 10.1016/j.jconrel.2008.04.014 [PubMed: 18538436]
21. Martello F, Piest M, Engbersen JF, Ferruti P. Effects of branched or linear architecture of bioreducible poly(amido amine)s on their in vitro gene delivery properties. *J Control Release.* 2012; 164:372–379. DOI: 10.1016/j.jconrel.2012.07.029 [PubMed: 22846986]
22. Neuberger P, Kichler A. Recent developments in nucleic acid delivery with polyethylenimines. *Adv Genet.* 2014; 88:263–288. DOI: 10.1016/B978-0-12-800148-6.00009-2 [PubMed: 25409609]

23. Scherer F, Schillinger U, Putz U, Stemberger A, Plank C. Nonviral vector loaded collagen sponges for sustained gene delivery in vitro and in vivo. *J Gene Med.* 2002; 4:634–643. [PubMed: 12439855]
24. Tyrone JW, et al. Collagen-embedded platelet-derived growth factor DNA plasmid promotes wound healing in a dermal ulcer model. *J Surg Res.* 2000; 93:230–236. [PubMed: 11027465]
25. Berry M, et al. Sustained effects of gene-activated matrices after CNS injury. *Mol Cell Neurosci.* 2001; 17:706–716. [PubMed: 11312606]
26. Patino MG, Neiders ME, Andreana S, Noble B, Cohen RE. Collagen as an implantable material in medicine and dentistry. *J Oral Implantol.* 2002; 28:220–225. [PubMed: 12498470]
27. Fang J, et al. Stimulation of new bone formation by direct transfer of osteogenic plasmid genes. *Proc Natl Acad Sci U S A.* 1996; 93:5753–8. [PubMed: 8650165]
28. Bonadio J, Smiley E, Patil P, Goldstein S. Localized, direct plasmid gene delivery in vivo: prolonged therapy results in reproducible tissue regeneration. *Nat Med.* 1999; 5:753–759. [PubMed: 10395319]
29. Bolander ME. Regulation of fracture repair by growth factors. *Proc Soc Exp Biol Med.* 1992; 200:165–170. [PubMed: 1374563]
30. Battegay EJ, Rupp J, Iruela-Arispe L, Sage EH, Pech M. PDGF-BB modulates endothelial proliferation and angiogenesis in vitro via PDGF beta-receptors. *J Cell Biol.* 1994; 125:917–928. [PubMed: 7514607]
31. Anusaksathien O, Webb SA, Jin QM, Giannobile WV. Platelet-derived growth factor gene delivery stimulates ex vivo gingival repair. *Tissue Eng.* 2003; 9:745–756. DOI: 10.1089/107632703768247421 [PubMed: 13678451]
32. Jiranek WA, et al. Production of cytokines around loosened cemented acetabular components. Analysis with immunohistochemical techniques and in situ hybridization. *J Bone Joint Surg Am.* 1993; 75:863–879. [PubMed: 8314826]
33. Pinheiro ML, et al. Quantification and localization of platelet-derived growth factor in gingiva of periodontitis patients. *J Periodontol.* 2003; 74:323–328. DOI: 10.1902/jop.2003.74.3.323 [PubMed: 12710751]
34. Salcetti JM, et al. The clinical, microbial, and host response characteristics of the failing implant. *Int J Oral Maxillofac Implants.* 1997; 12:32–42. [PubMed: 9048452]
35. Yu X, Hsieh SC, Bao W, Graves DT. Temporal expression of PDGF receptors and PDGF regulatory effects on osteoblastic cells in mineralizing cultures. *Am J Physiol.* 1997; 272:C1709–1716. [PubMed: 9176163]
36. Saygin NE, Tokiyasu Y, Giannobile WV, Somerman MJ. Growth factors regulate expression of mineral associated genes in cementoblasts. *J Periodontol.* 2000; 71:1591–1600. DOI: 10.1902/jop.2000.71.10.1591 [PubMed: 11063392]
37. Hsieh SC, Graves DT. Pulse application of platelet-derived growth factor enhances formation of a mineralizing matrix while continuous application is inhibitory. *J Cell Biochem.* 1998; 69:169–180. [PubMed: 9548564]
38. Marzouk KM, Gamal AY, Al-Awady AA, Sharawy MM. Platelet-derived growth factor BB treated osteoprogenitors inhibit bone regeneration. *J Oral Implantol.* 2008; 34:242–247. DOI: 10.1563/1548-1336(2008)34[243:PGFBTO]2.0.CO;2 [PubMed: 19170289]
39. Evans CH. Gene therapy for bone healing. *Expert Rev Mol Med.* 2010; 12:e18. [PubMed: 20569532]
40. Zhang Z, Chen J, Jin D. Platelet-derived growth factor (PDGF)-BB stimulates osteoclastic bone resorption directly: the role of receptor beta. *Biochem Biophys Res Commun.* 1998; 251:190–194. DOI: 10.1006/bbrc.1998.9412 [PubMed: 9790928]
41. Pierce GF, et al. Platelet-derived growth factor and transforming growth factor-beta enhance tissue repair activities by unique mechanisms. *J Cell Biol.* 1989; 109:429–440. [PubMed: 2745556]
42. Kubota K, Sakikawa C, Katsumata M, Nakamura T, Wakabayashi K. Platelet-derived growth factor BB secreted from osteoclasts acts as an osteoblastogenesis inhibitory factor. *J Bone Miner Res.* 2002; 17:257–265. DOI: 10.1359/jbmr.2002.17.2.257 [PubMed: 11811556]
43. Anusaksathien O, Jin Q, Zhao M, Somerman MJ, Giannobile WV. Effect of sustained gene delivery of platelet-derived growth factor or its antagonist (PDGF-1308) on tissue-engineered

- cementum. *J Periodontol.* 2004; 75:429–440. DOI: 10.1902/jop.2004.75.3.429 [PubMed: 15088882]
44. de Costa AM, et al. An experimental model for the study of craniofacial deformities. *Acta Cir Bras.* 2010; 25:264–268. [PubMed: 20498939]
45. Sculean A, Chapple IL, Giannobile WV. Wound models for periodontal and bone regeneration: the role of biologic research. *Periodontol 2000.* 2015; 68:7–20. DOI: 10.1111/prd.12091 [PubMed: 25867976]
46. Gomes PS, Fernandes MH. Rodent models in bone-related research: the relevance of calvarial defects in the assessment of bone regeneration strategies. *Lab Anim.* 2011; 45:14–24. DOI: 10.1258/la.2010.010085 [PubMed: 21156759]
47. Park CH, et al. Tissue engineering bone-ligament complexes using fiber-guiding scaffolds. *Biomaterials.* 2012; 33:137–145. [PubMed: 21993234]
48. Jin QM, Anusaksathien O, Webb SA, Rutherford RB, Giannobile WV. Gene therapy of bone morphogenetic protein for periodontal tissue engineering. *J Periodontol.* 2003; 74:202–213. DOI: 10.1902/jop.2003.74.2.202 [PubMed: 12666709]
49. Schneider CA, Rasband WS, Eliceiri KW. NIH Image to ImageJ: 25 years of image analysis. *Nat Methods.* 2012; 9:671–675. [PubMed: 22930834]

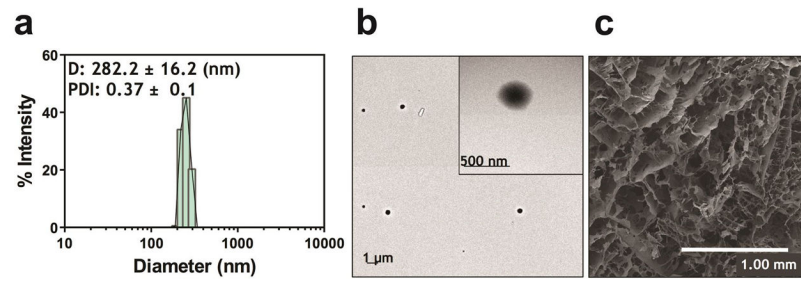


Figure 1. Representative size distribution diagram of PEI-pPDGF polyplexes as determined using Zetasizer Nano (a) and TEM image of PEI-pPDGF polyplexes prepared at a N:P ratio of 10 (scale bar = 1 μm; inset scale bar = 500 nm) (b) and SEM image of a collagen scaffold (scale bar = 1.00 mm)(c).

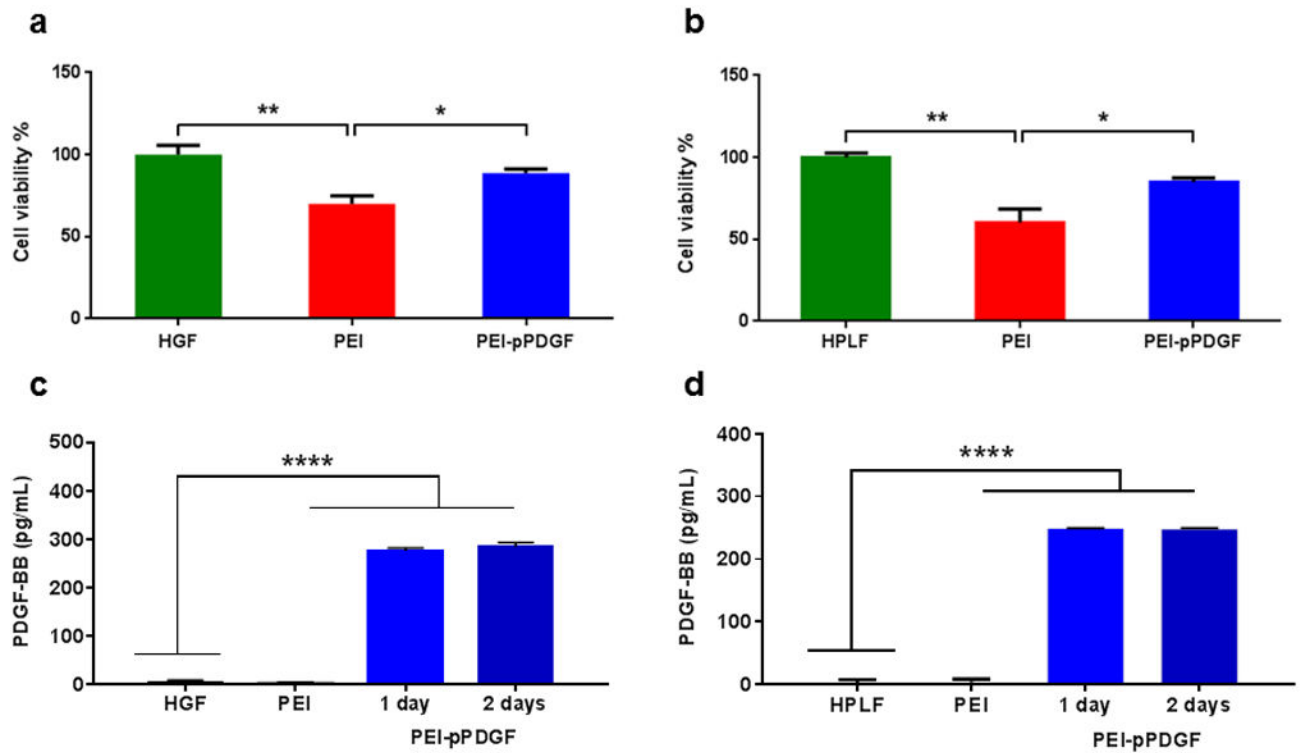


Figure 2.

Effects of PEI-pPDGF polyplexes fabricated at N/P ratio of 10 (1 μ g pPDGF) on hGF (a) and hPLF (b) cells after 48 h. Significant differences between the treatments and the untreated cells were assessed by one-way analysis of variance followed by Tukey's post-test (* $p < 0.05$; ** $p < 0.01$). Values are expressed as mean \pm SD ($n = 4$). ELISA assay demonstrating the expression of PDGF-BB protein from hGF (c) and hPLF (d) cells at 24 and 48 hours, post transfection with PEI-pPDGF polyplexes (Prepared at an N/P ratio of 10 (1 μ g pPDGF)). Significant differences between PEI-pPDGF, cells treated with PEI and untreated cells were assessed by one-way analysis of variance followed by Tukey's post-test (**** $p < 0.0001$). Values are expressed as mean \pm SD ($n = 4$).

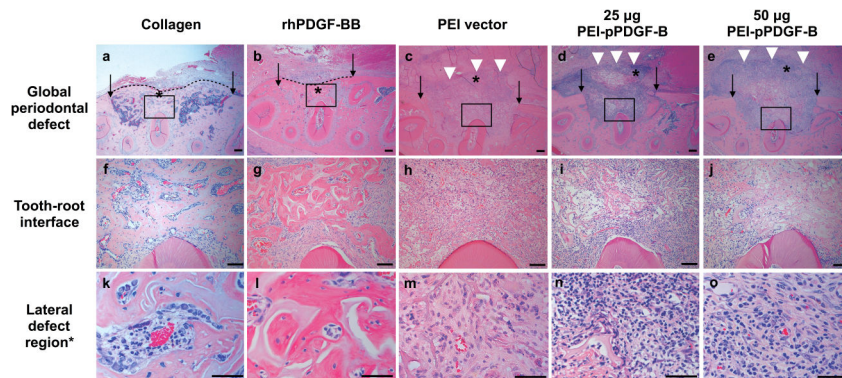


Figure 3.

Sustained PDGF delivery inhibits periodontal wound healing in vivo. Histologic images of surgically-created periodontal defects at 21d after treatment with collagen scaffold alone or with PDGF protein, low- and high-dose PEI-pPDGF-B gene therapy complex, or PEI vector alone. The top panel (a–e) shows the defect at 20x original magnification, with the original defect borders represented by arrows. Significantly more bridging bone across the defect (dotted line) was found for collagen and collagen plus PDGF protein groups. A robust inflammatory infiltrate was noted lateral to the defect (white arrowheads) for the PDGF gene therapy groups and PEI vector control group. The center row (f–j) shows the prepared tooth root at 100x original magnification. In images f and g, the collagen and PDGF group have bone fill within the defect, also shown at higher magnification in panels k and l. The bottom row (k–o) shows features at high magnification (400x). In the gene therapy and vector control groups, residual scaffold material is indicated by an asterisk. In these groups, a high-magnification view of the inflammatory infiltrate is seen in images m, n, o.

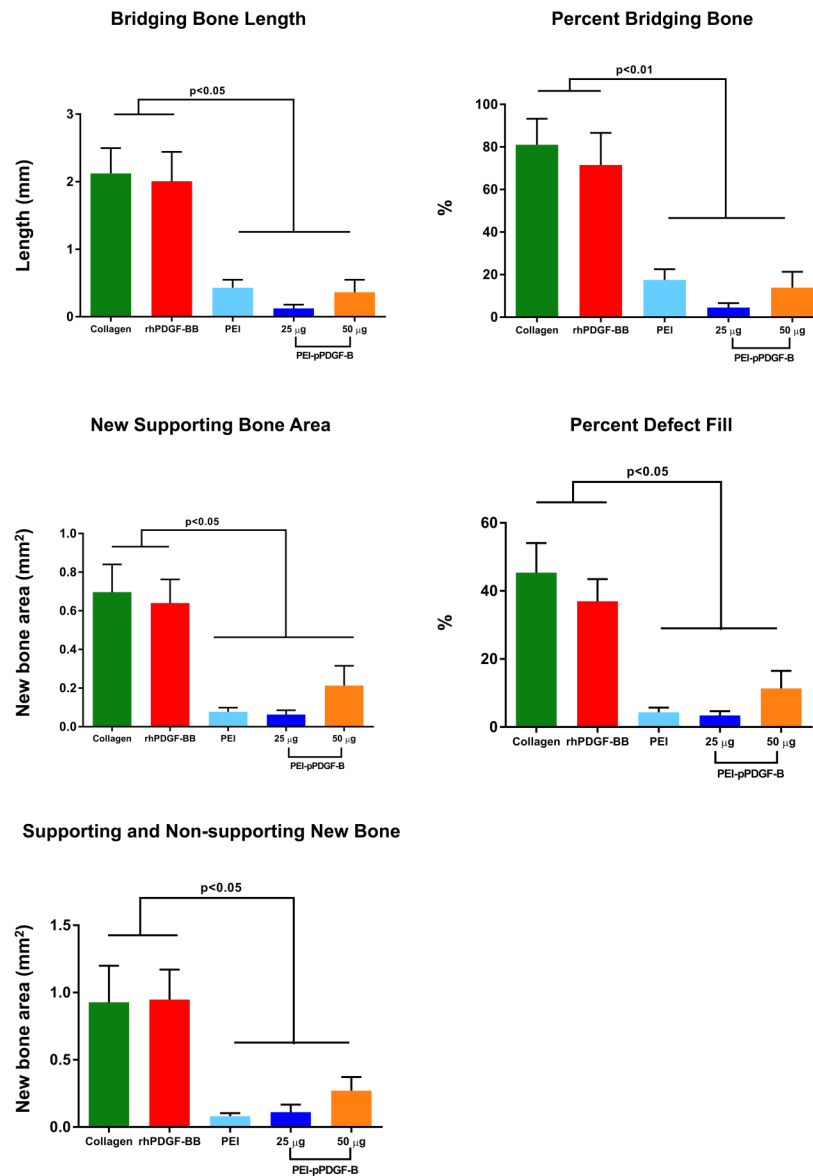


Figure 4. PDGF gene therapy and PEI vector inhibit bone bridging length across the defect and new bone area within the defect. Histomorphometric analysis is shown for bridge length (mm) across the defect (**a**) and bridging bone as percent of original defect length (**b**). Area measurements include new bone within surgically-created defect in mm² (**c**), defect fill as percentage of original defect area (**d**), and total new bone (mm²), including that external to the original defect (**e**). Significant differences between groups were assessed by one-way analysis of variance followed by Tukey's post-test (* $p < 0.05$, ** $p < 0.01$, *** $p < 0.001$, **** $p < 0.0001$). Values are expressed as mean \pm SEM.

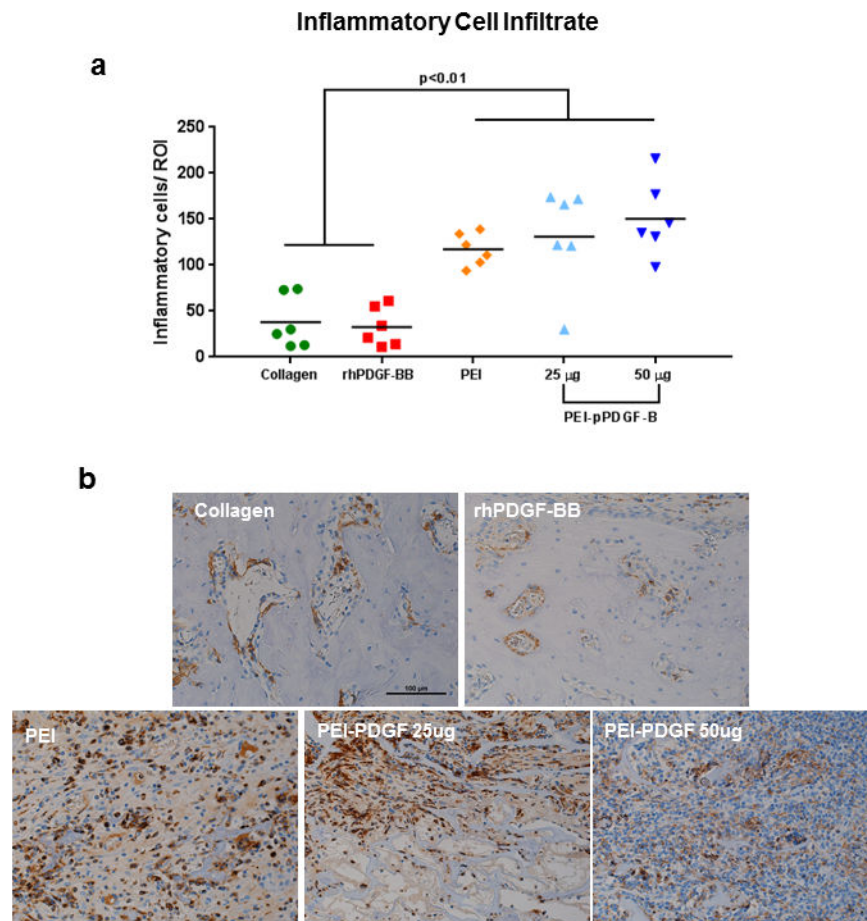


Figure 5.

PEI gene therapy and vector delivery stimulates inflammation in the lateral defect region. Inflammatory cells were evaluated in four regions of interest (ROI) per specimen: lateral-defect, peri-root, and the average of two peri-defect ROIs. The inflammatory cells counted within each ROI were lymphocyte-like, macrophage-like and polymorphonuclear-like cells. At least five-times greater inflammatory cells were present in the lateral defect region compared with other regions. Significantly more inflammatory cells were found in the 25 and 50 µg PEI-pPDGF-B groups and PEI vector group when compared with the collagen and rhPDGF-B groups (**a**). Statistical analysis performed was one-way analysis of variance with Tukey's *post hoc* test (* $p < 0.05$, ** $p < 0.01$, *** $p < 0.001$, **** $(p < 0.0001)$). Immunohistochemistry staining for CD68, a marker for macrophages and monocytes, was used to confirm cells were inflammatory cells. The lateral defect ROI is shown in panel (**b**). Representative samples from collagen only group, PEI alone, rhPDGF-BB, PEI-pPDGF-B 25µg and PEI-pPDGF-B 50µg groups are shown (**b**). Note that the PEI-PDGF 50 µg group demonstrated abundant CD68 positive cells in the lateral area to the bone defect. These images were obtained using the same magnification (20X).

Table 1

Length of surgically created defects and prepared roots and newly-formed cementum at 21 days after defect creation.

Periodontal alveolar bone defects were of uniform length between groups ($p > 0.05$) and PEI vector inhibit bone bridging length across the defect and new bone area within the defect. Histomorphometric analysis for bridging bone shown as a percent of the original defect length (**a**) and bridge length (mm) across the defect (**b**). Area measurements include new bone within the surgically-created defect in mm^2 (**c**), defect fill as a percentage of original defect area (**d**), and total new bone (mm^2), including that external to the original defect (**e**). Significant differences between groups were assessed by one-way analysis of variance followed by Tukey's post-test ($*p < 0.05$, $**p < 0.01$, $***p < 0.001$, $****p < 0.0001$). Values are expressed as mean \pm SEM.

Group	Defect Length (mm)	Root preparation defect (mm)	Cementum (mm)
Collagen	2.57 \pm 0.44	0.7 \pm 0.3	0.11 \pm 0.16 ^c
rhPDGF-BB	2.80 \pm 0.31	1.02 \pm 0.27 ^a	0.15 \pm 0.15 ^d
PEI vector	2.54 \pm 0.46	1.10 \pm 0.57 ^b	0.00 \pm 0.00 ^f
25 μg PEI-pPDGF-B	2.64 \pm 0.35	0.37 \pm 0.26 ^{a,b}	0.15 \pm 0.11 ^e
50 μg PEI-pPDGF-B	2.64 \pm 0.40	0.7 \pm 0.22	0.54 \pm 0.24 ^{c,d,e,f}

Abbreviations: PDGF-B, platelet-derived growth factor-B; PEI, polyethylenimine.

^{a-f} Similar letters indicate statistically significant difference between groups (1 way-ANOVA and Tukey's *post hoc*).